Supplement of Geosci. Model Dev., 10, 721–750, 2017
http://www.geosci-model-dev.net/10/721/2017/
doi:10.5194/gmd-10-721-2017-supplement

Geoscientific Model Development
Open Access

Supplement of

The high-resolution version of TM5-MP for optimized satellite retrievals: description and validation

Jason E. Williams et al.

Correspondence to: Jason E. Williams (williams@knmi.nl)

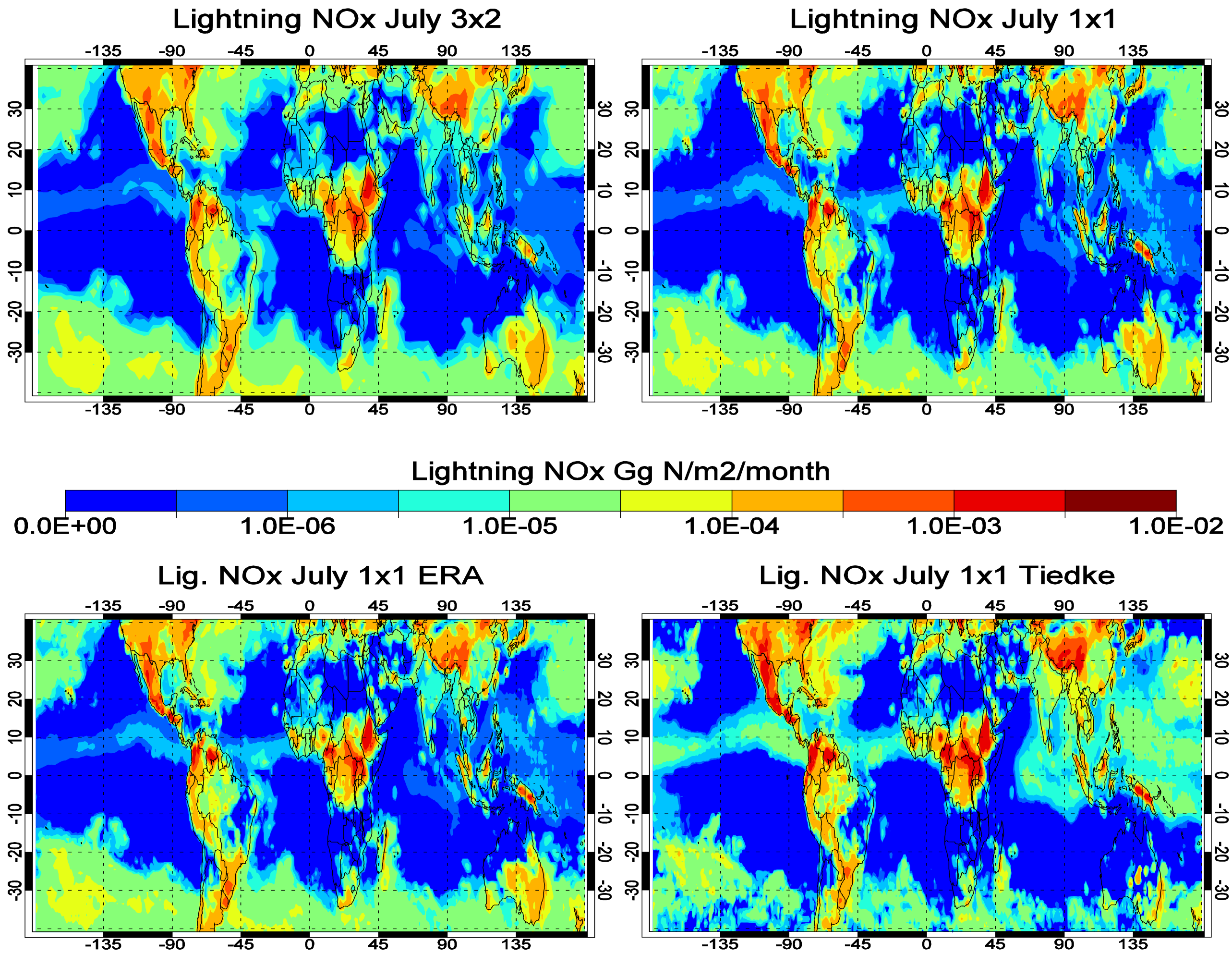

Figure S1a: The global distribution of lightning NO_x emissions for July 2006 at ~400hPa for the 3º x 2º (top left) and 1º x 1º (top right) simulations. The corresponding distribution of lightening NO_x using the Tiedke (1989) scheme is also shown bottom right. Fluxes are given in Gg N/m2/month.

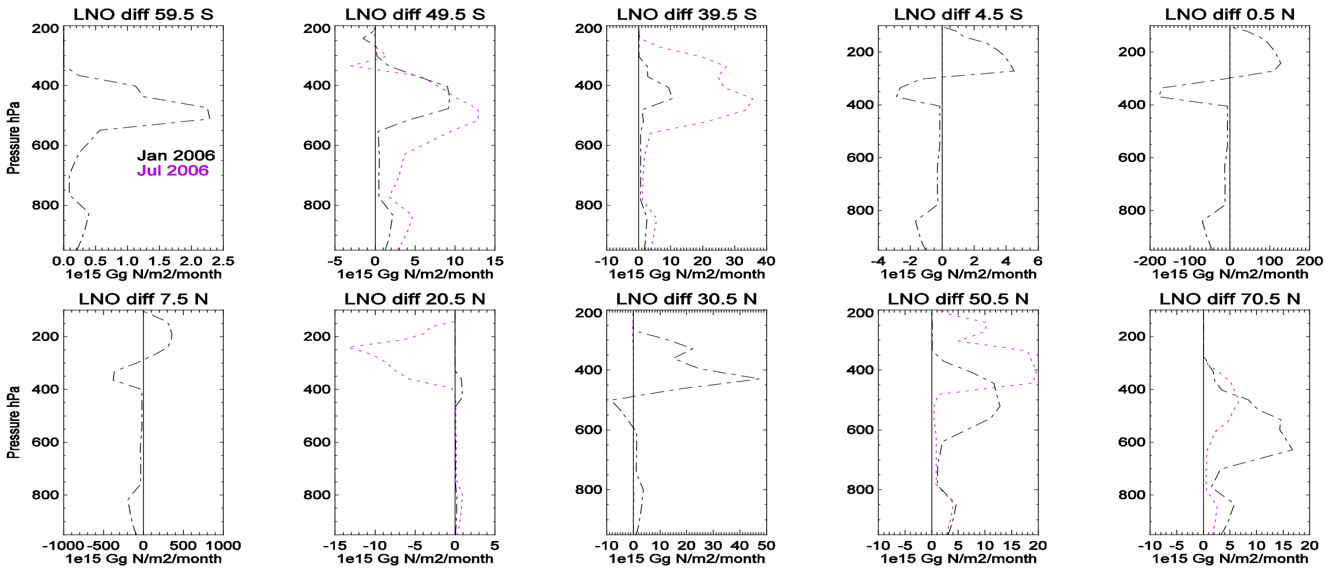

Figure S1b: 1-D profiles of the absolute differences in Lightning NO emissions calculated by the parameterization of Meijer et al. (2001) between those calculated using Tiedtke and ERA-interim for various latitudes at 0.5ºE. Absolute differences are equal to ERA-Tiedtke, and shown for both January and July, being given in Gg N m^2 month and subsequently scaled up by 1.0e15 for visualization.

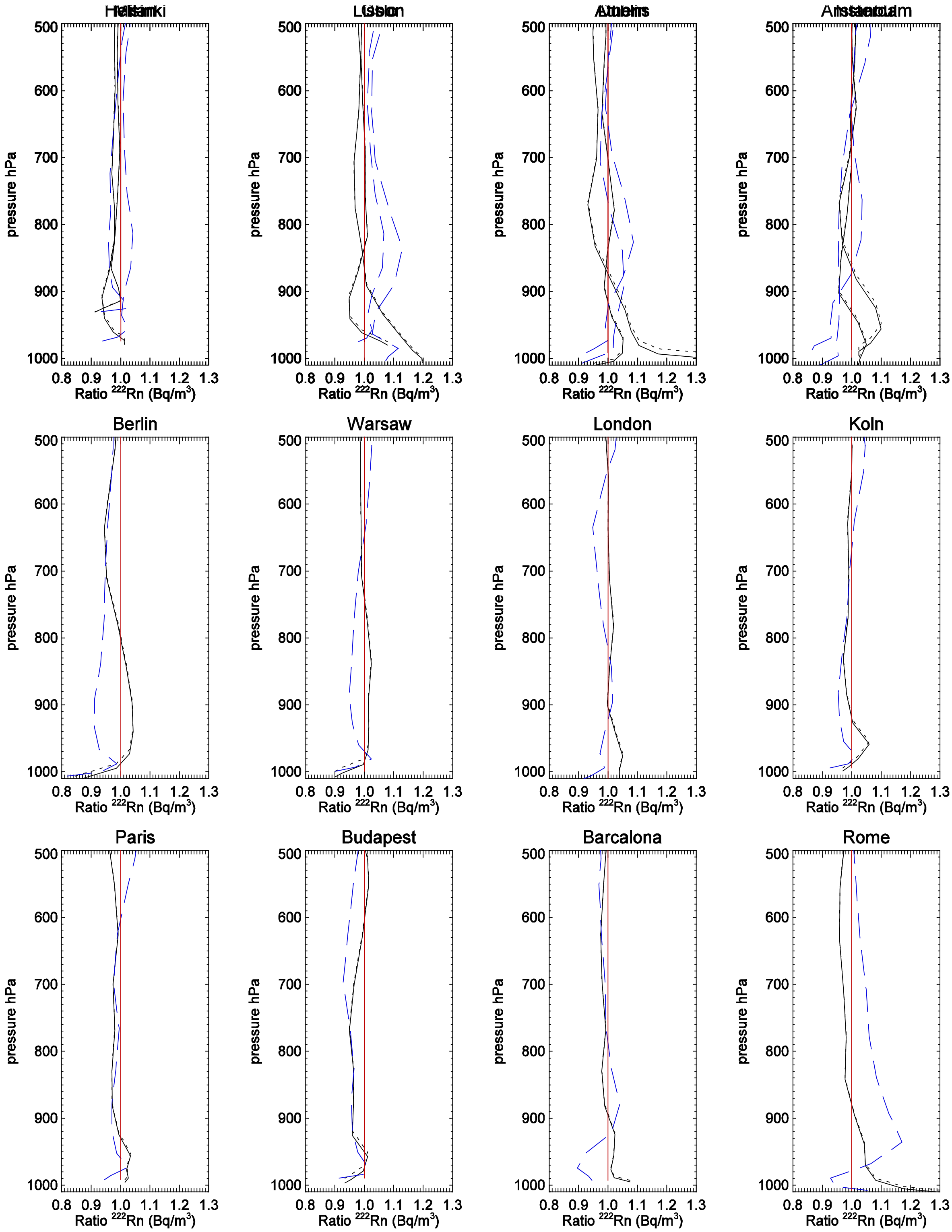

Figure S2: Ratios of the vertical profiles of ^{222}Rn between 1º x1º /3º x 2º simulations above selected European cities for January (black) and July (Blue) in 2006. The red line represents the ideal ratio of 1.0 throughout the column.

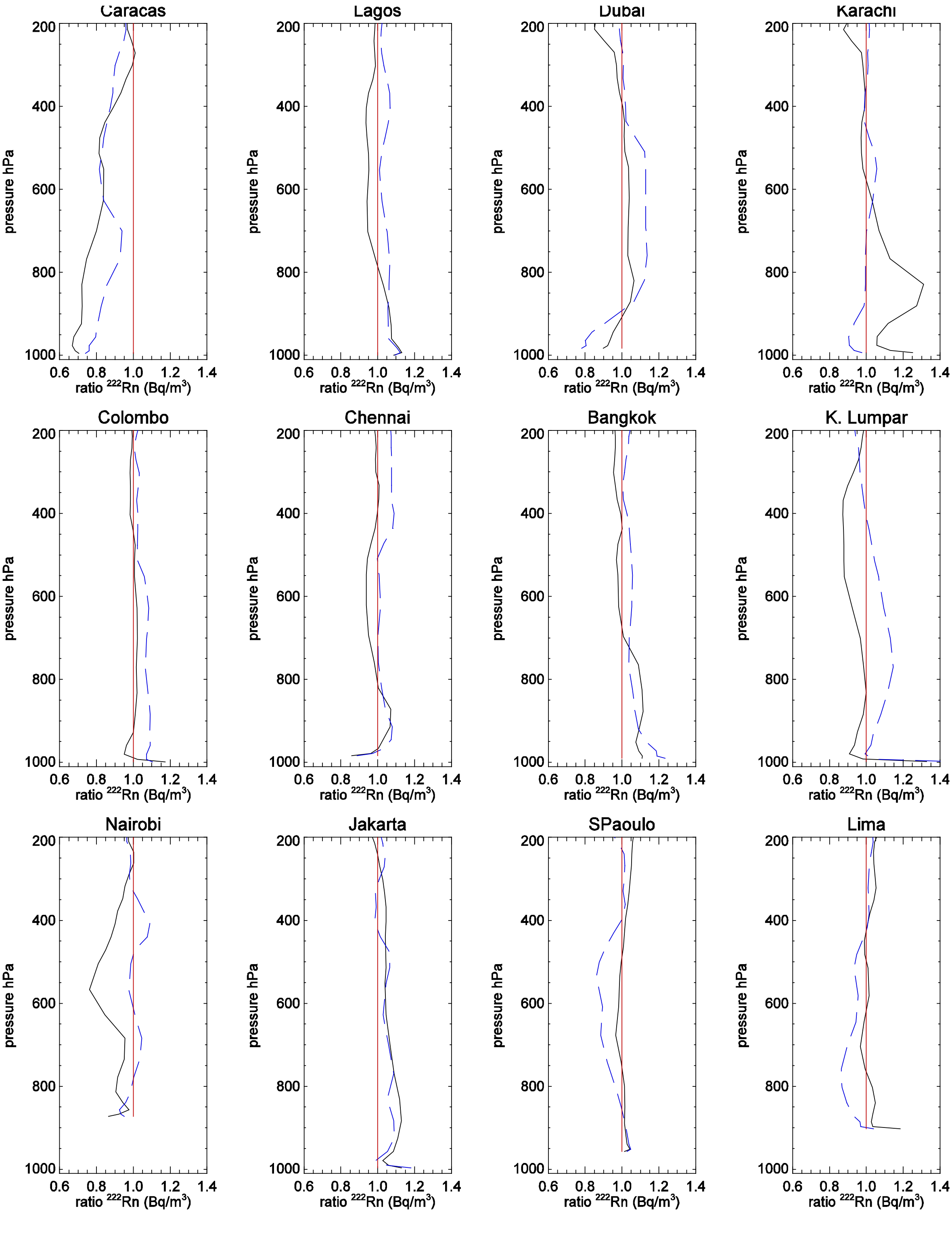

Figure S3: Ratios of the vertical profiles of ^{222}Rn between 1º x1º /3º x 2º simulations above selected Tropical cities for January (black) and July (Blue) in 2006. The red line represents the ideal ratio of 1.0 throughout the column.

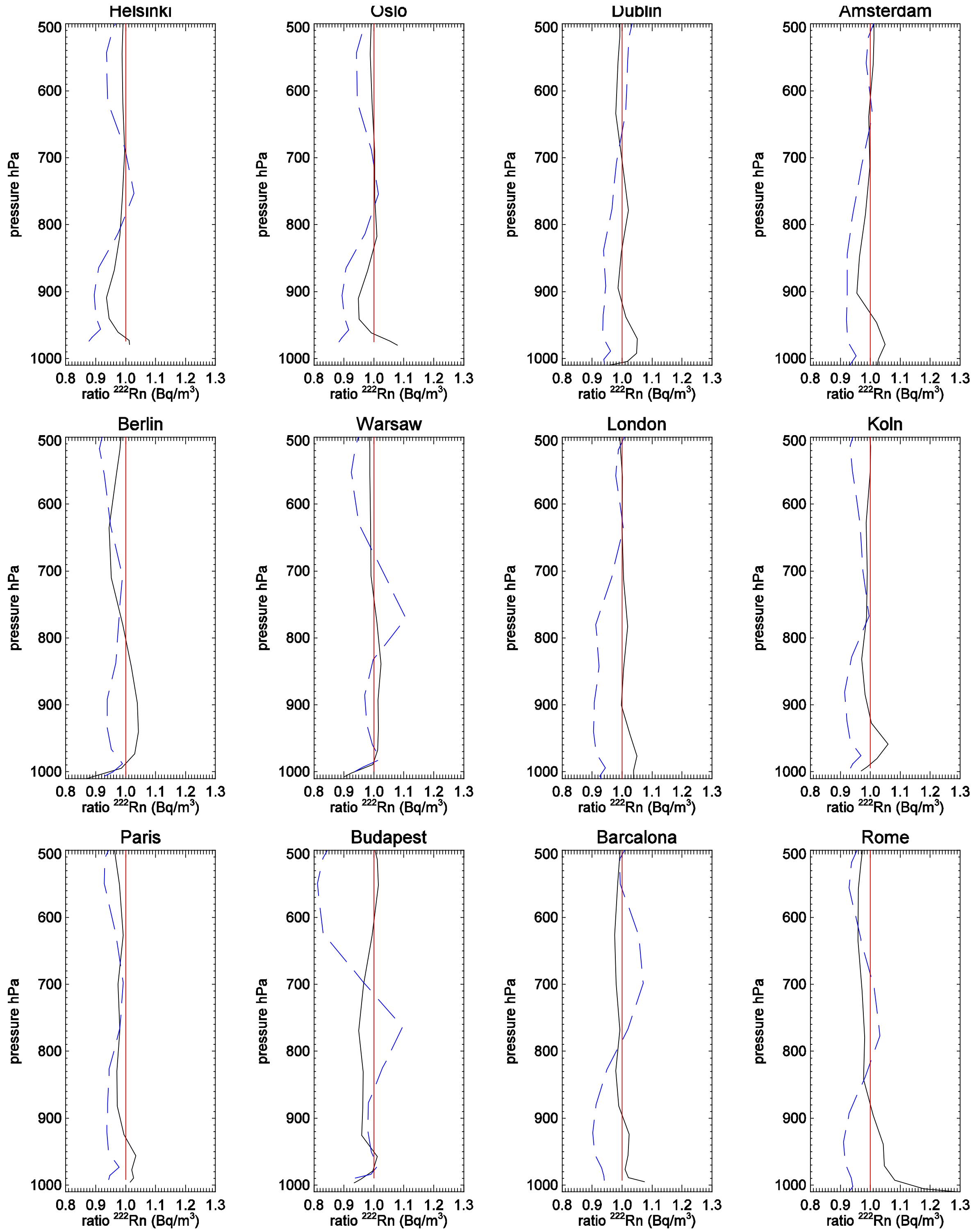

Figure S4: Ratios of the vertical profiles of ^{222}Rn above selected European cities for January (black) and July (Blue) during 2006. The ratio is representative of 1º x1º /1º x 1º (Tiedke). The red-line represents the ideal ratio of 1.0 throughout the column.

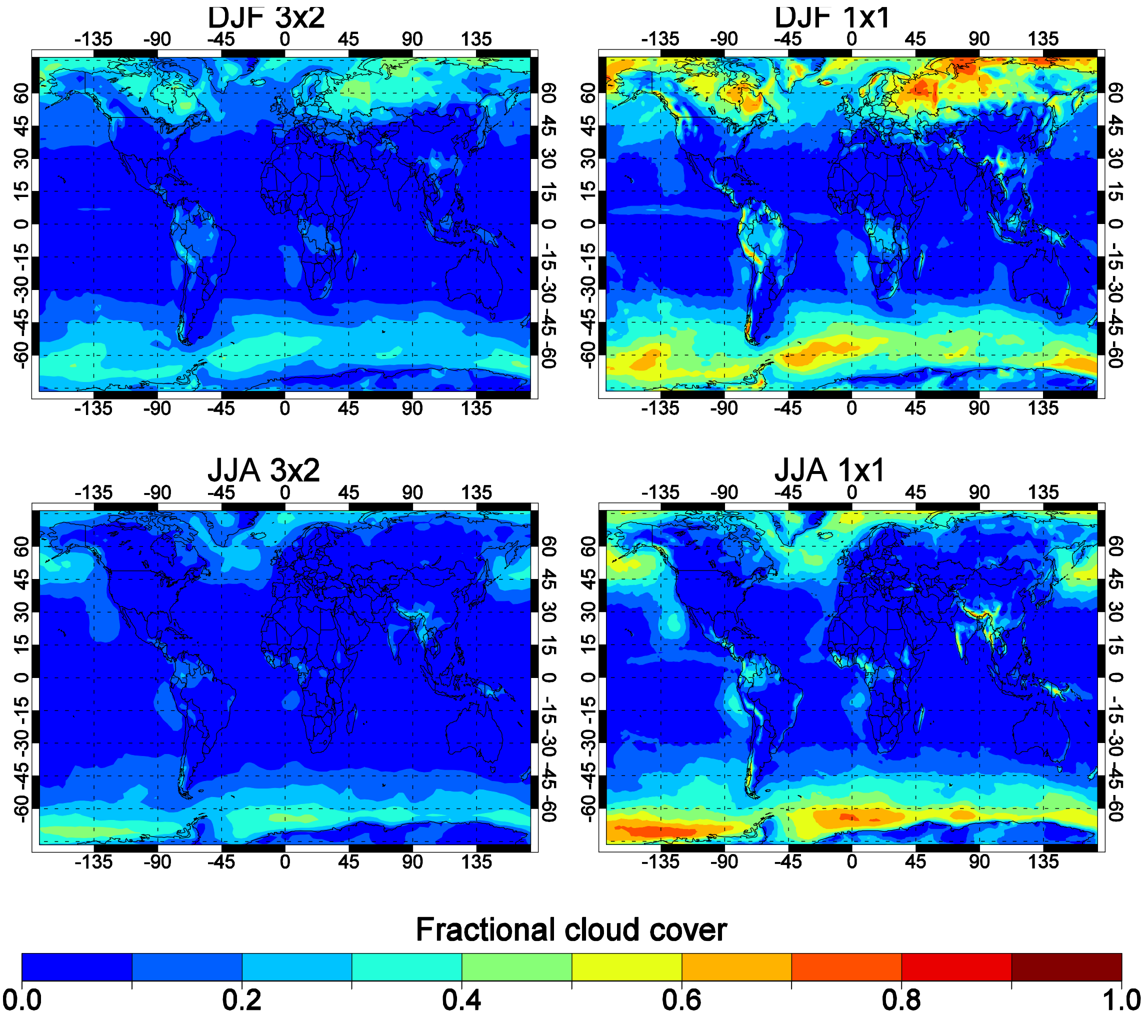

Figure S5: Comparisons of seasonal mean cloud cover values at the top of the boundary layer for (top) DJF and (bottom) JJA between the 3º x 2º (left) and 1º x 1º (right) simulations. The values shown are representative of 1-2 km of the troposphere, which exhibits high cloud incidence.

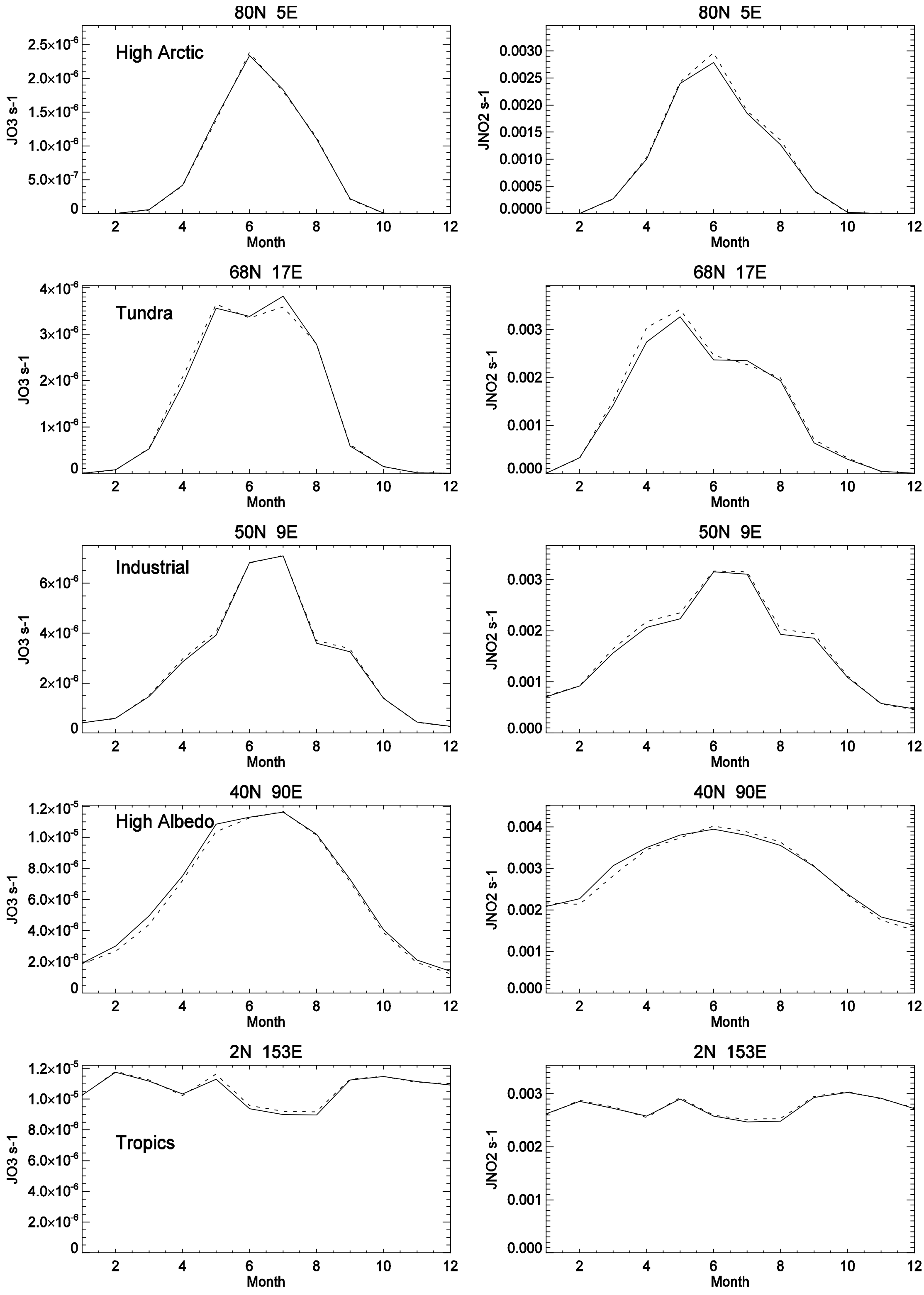

Figure S6: Comparisons of monthly mean J_{O3} (left) and J_{NO2} (right) values at the surface between the 3º x 2º (solid line) and 1º x 1º (dashed line) simulations. The locations selected are identical to those shown in Williams et al. (2012), where the type of region is given in each panel to the left**.**

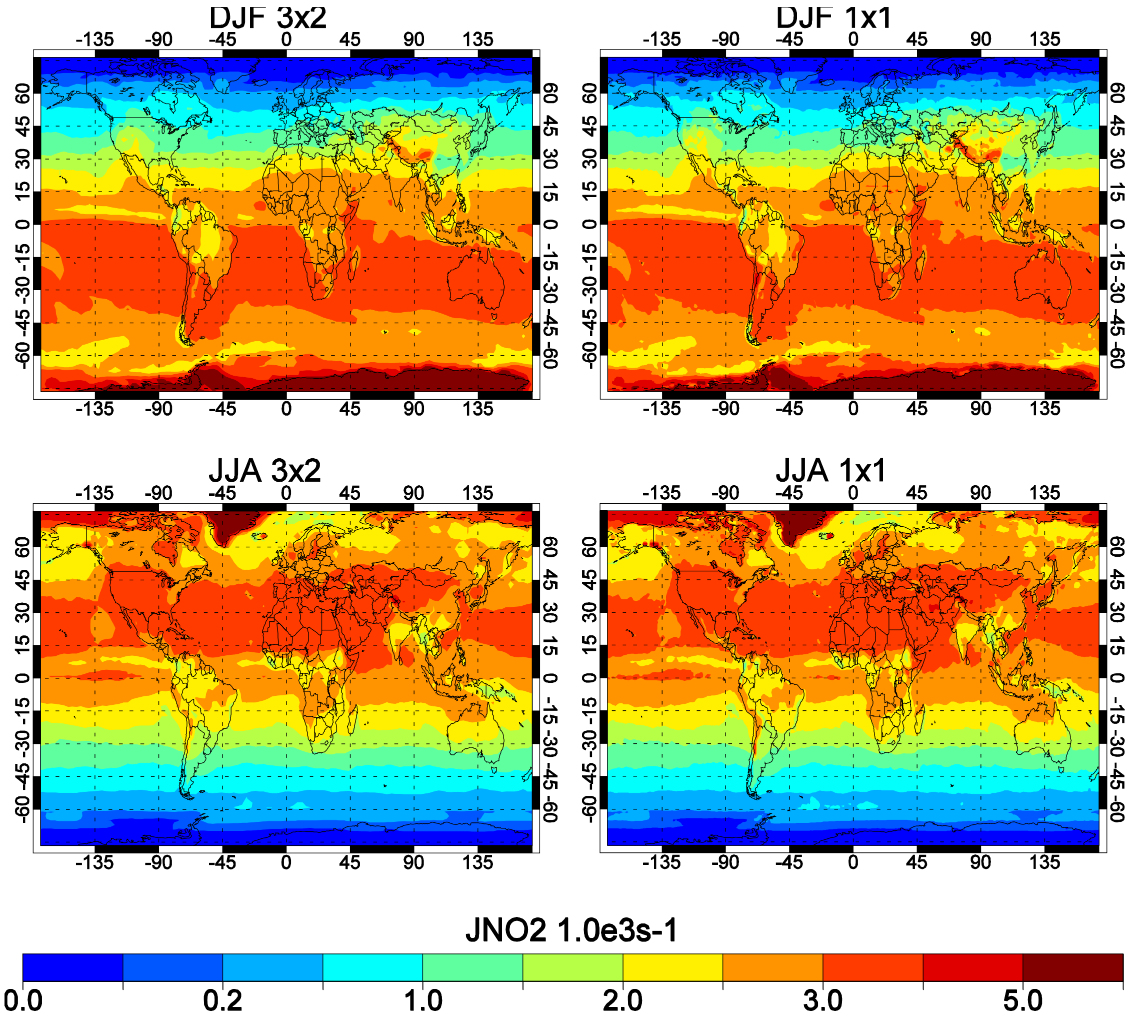

Figure S7: Comparisons of near-surface seasonal mean J_{NO2} values for (top) DJF and (bottom) JJA between the 3º x 2º (left) and 1º x 1º (right) simulations. The values shown are representative of the lowest km of the troposphere.

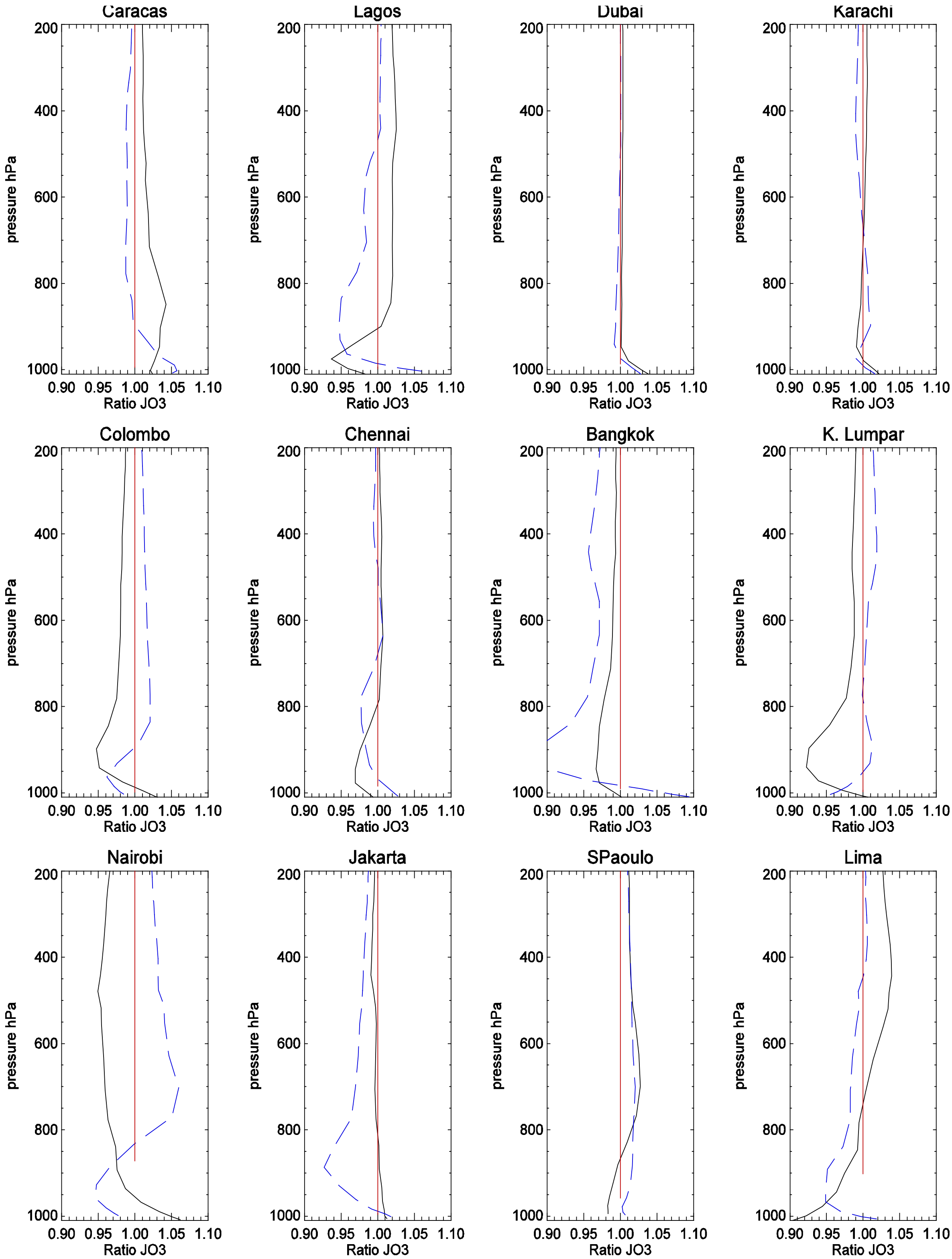

Figure S8a: Comparisons of the ratio of monthly mean J_{O3} profiles above selected tropical cities for January (black) and July (Blue) in 2006. The ratio is equal to 1º x 1º / 3º x 2º values.

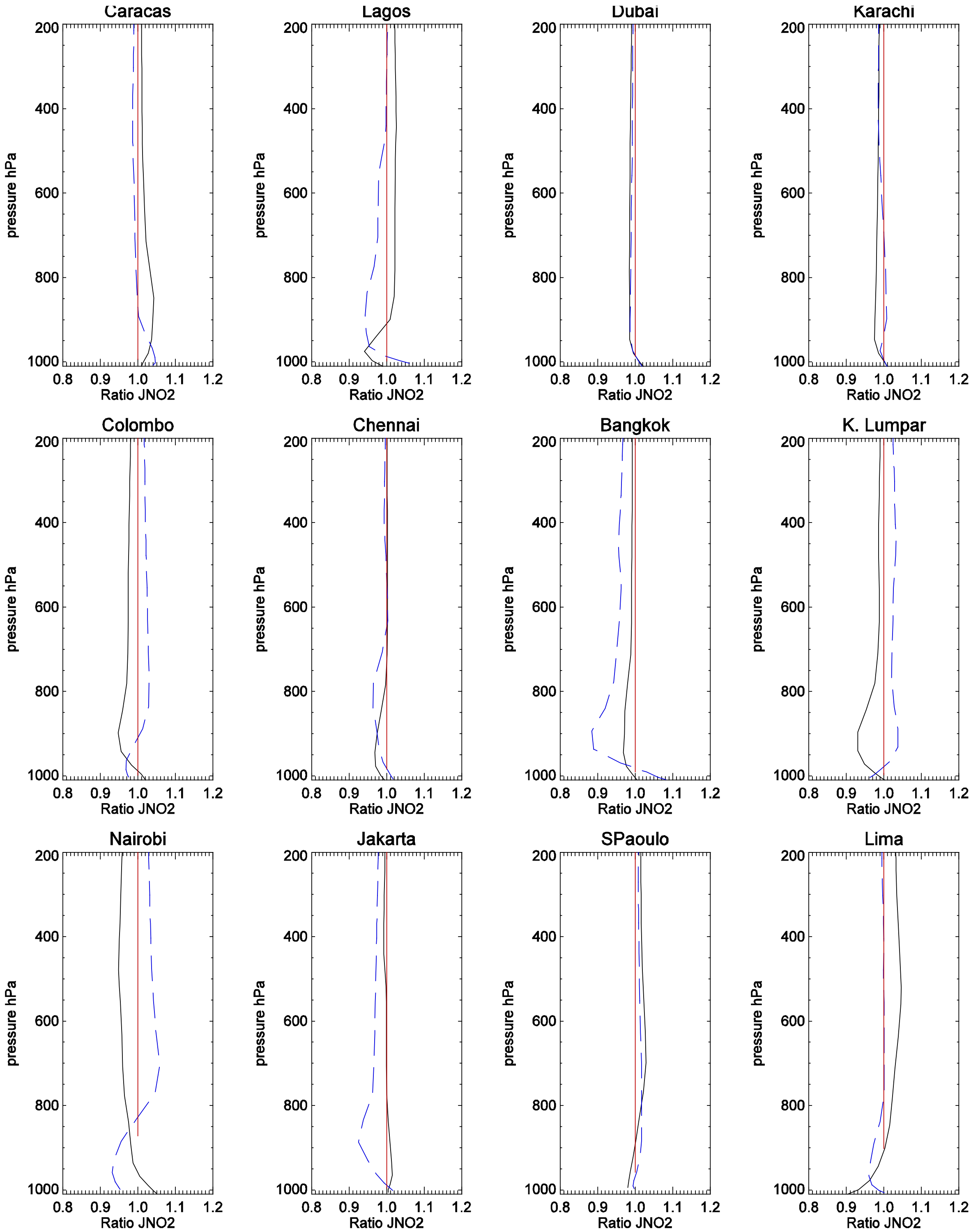

Figure S8b: Comparisons of the ratio of monthly mean J_{NO2} profiles above selected tropical cities for January (black) and July (Blue) in 2006. The ratio is equal to 1º x 1º / 3º x 2º values.

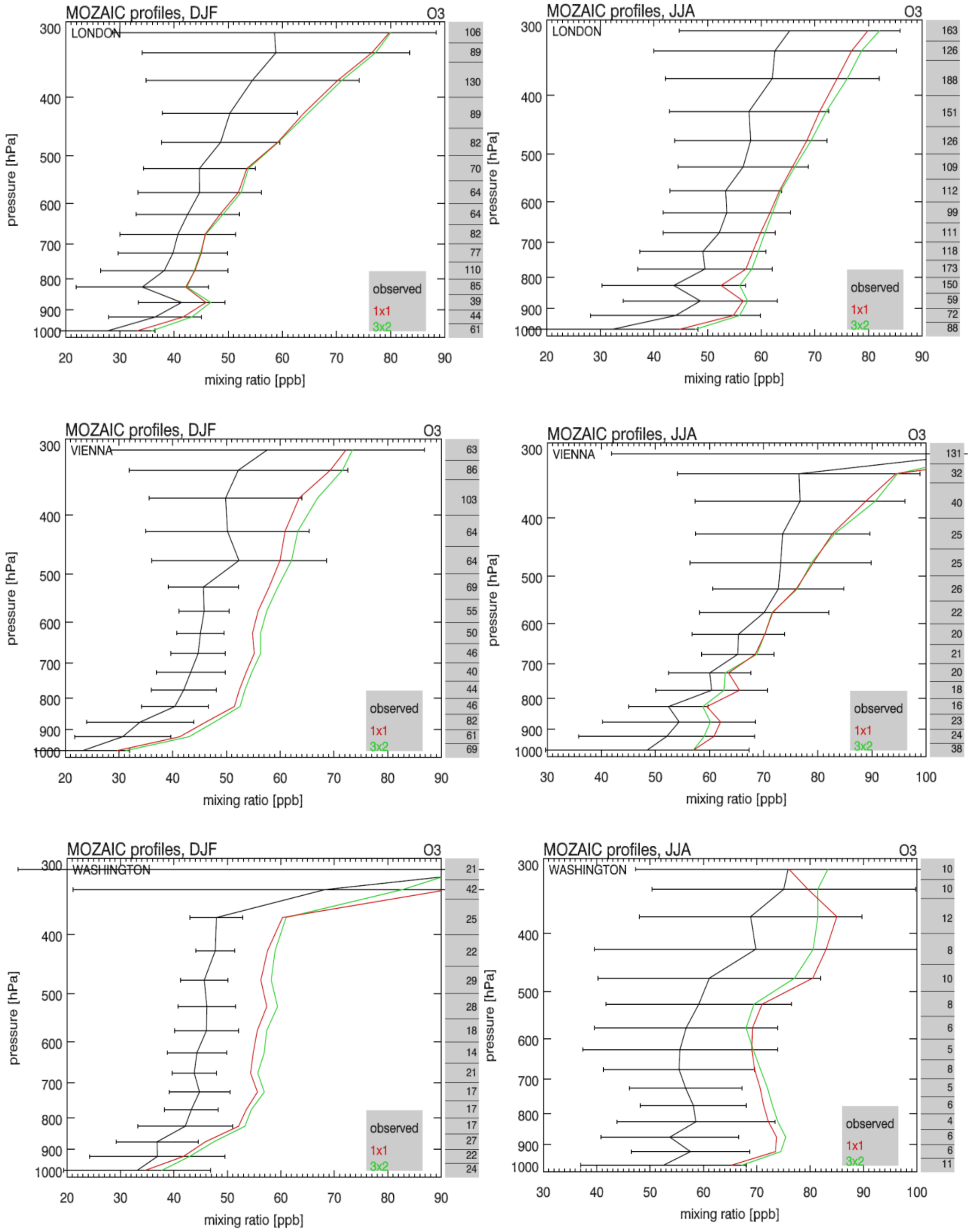

Figure S9a: Seasonal comparisons of tropospheric O_3 profiles (ppb) taken as part of the MOZIAC flight program for (left) DJF and (right) JJA for (top) London, (middle) Vienna and (bottom) Washington.

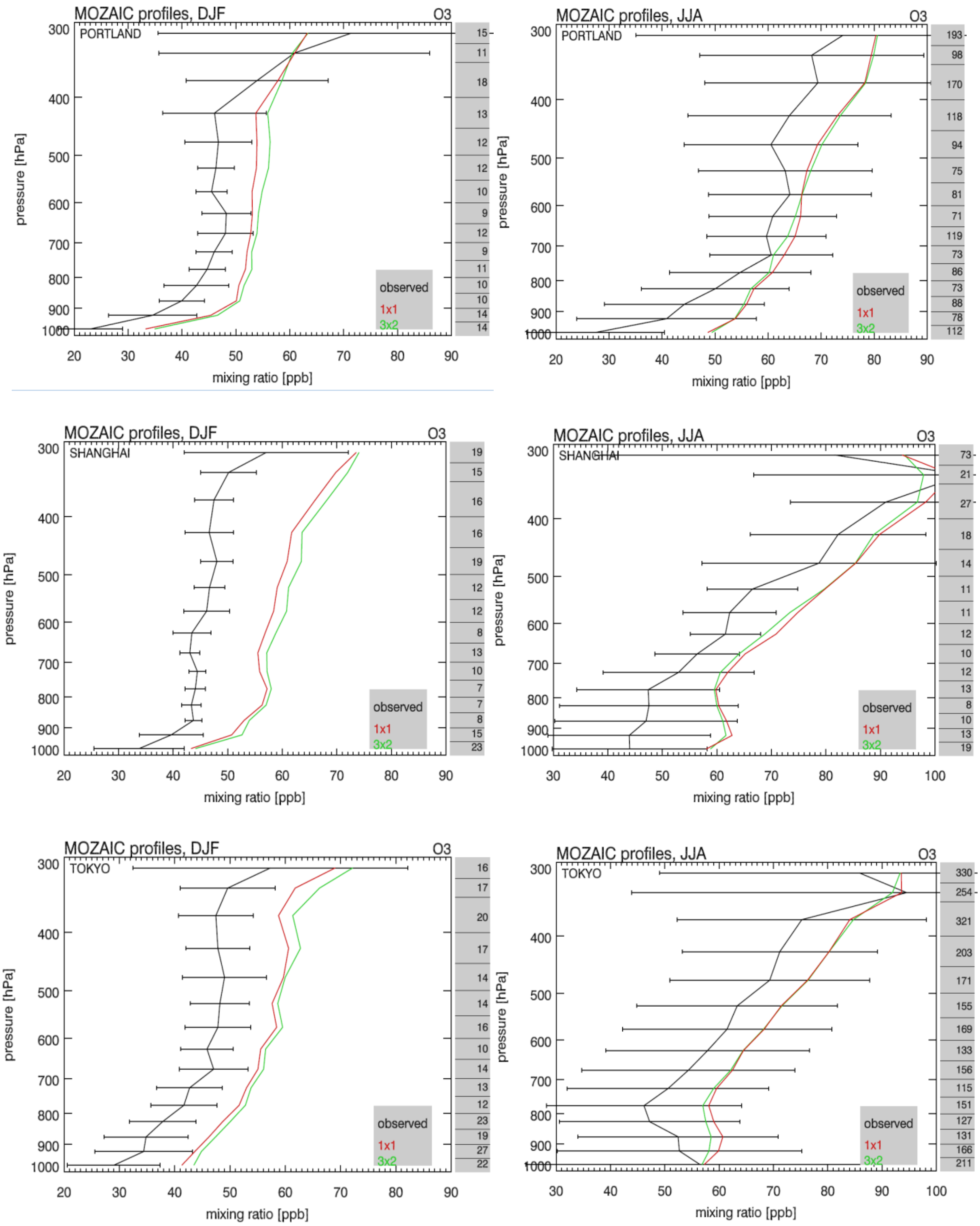

Figure S9b: As for Fig. S9a except for Portland (top), Shanghai (middle) and Tokyo (bottom).

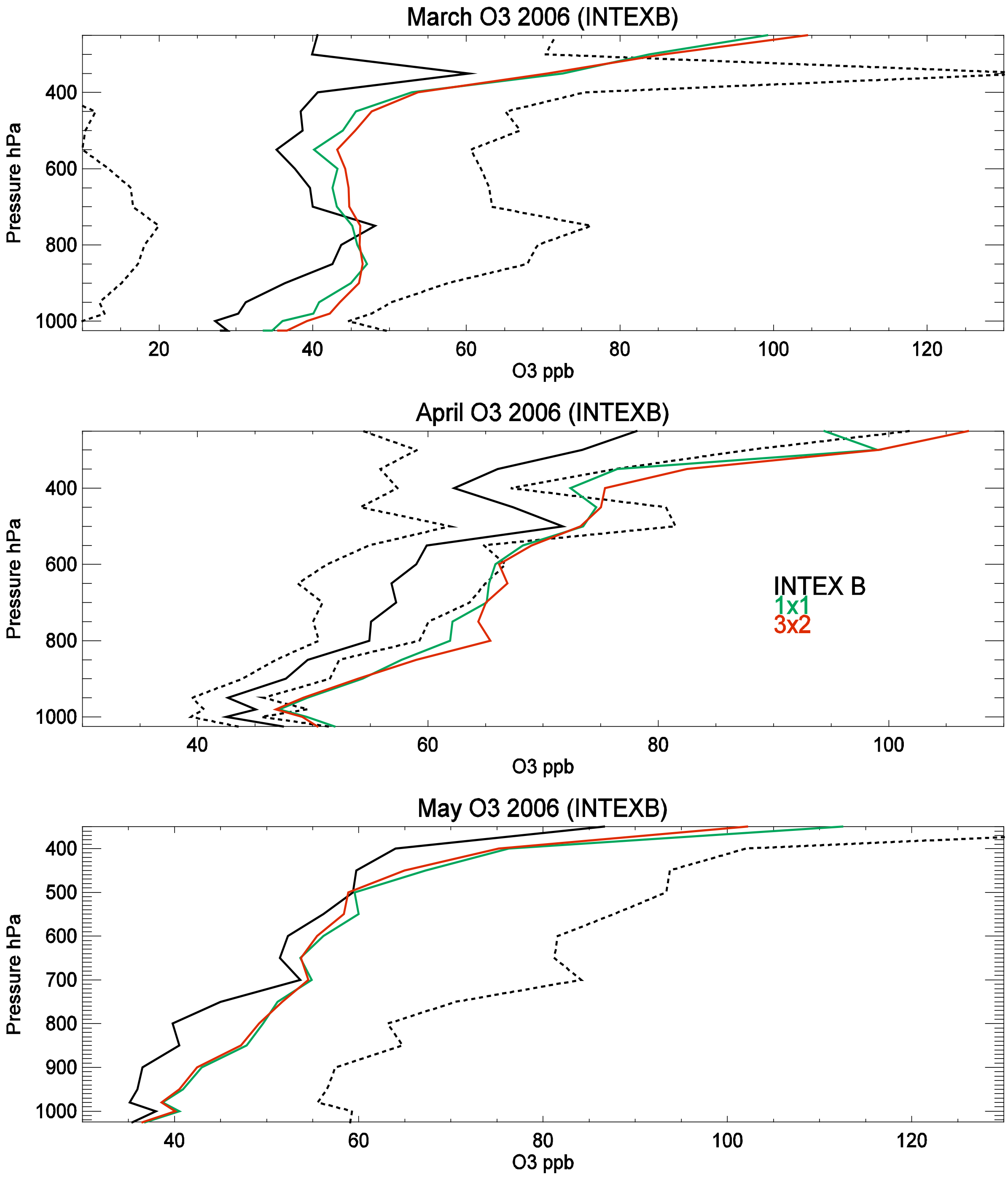

Figure S10: Comparisons of monthly composites of tropospheric O_3 profiles (ppb) against measurements taken during the INTEX-B campaign between March and May 2006 for both 3º x 2º and 1º x 1º simulations. The dotted line represents the 1-σ variability associated with the measurements.

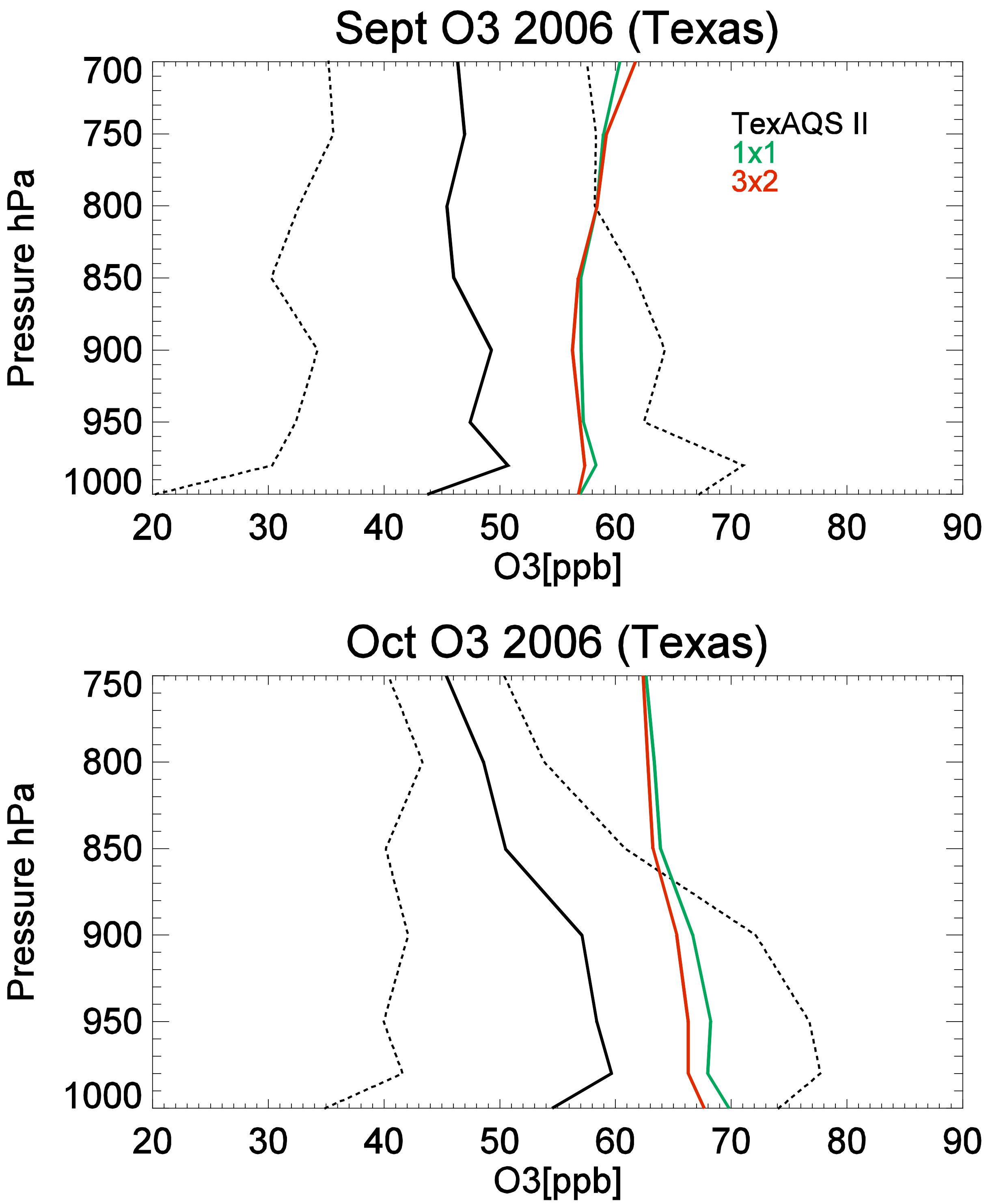

Figure S11: Comparisons of monthly tropospheric O_3 profiles assembled from data taken during September and October 2006 as part of the Texas-AQS measurement campaign. The dotted line represents the 1-σ variability associated with the measurements. For details of the flight paths the reader is referred to the details given in Parrish et al. (2009).

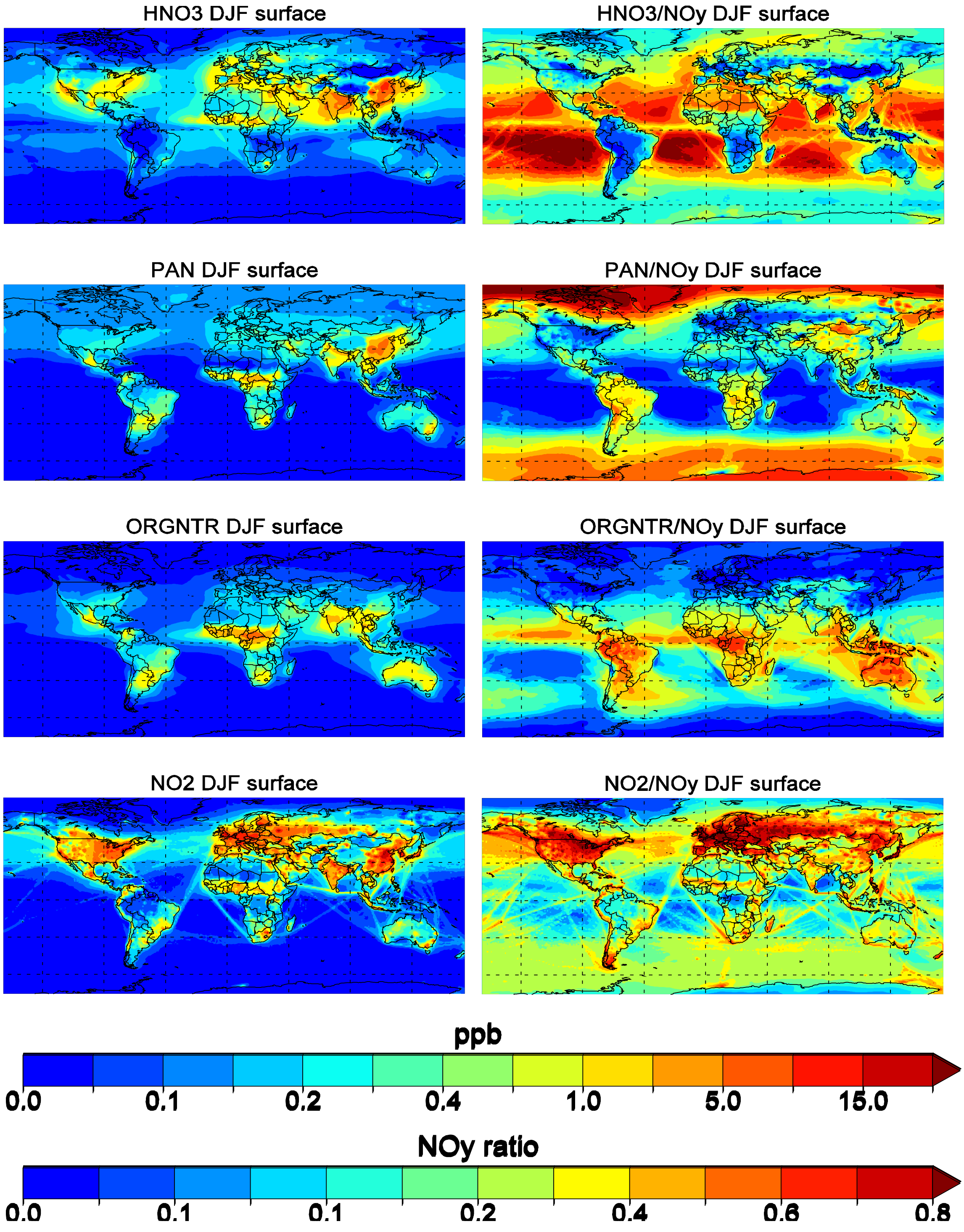

Figure S12: The horizontal mean distribution of (top to bottom) HNO_3, PAN, ORGNTR and NO_2 in the 1° x 1° simulation for DJF, along with the corresponding NO_y ratios.

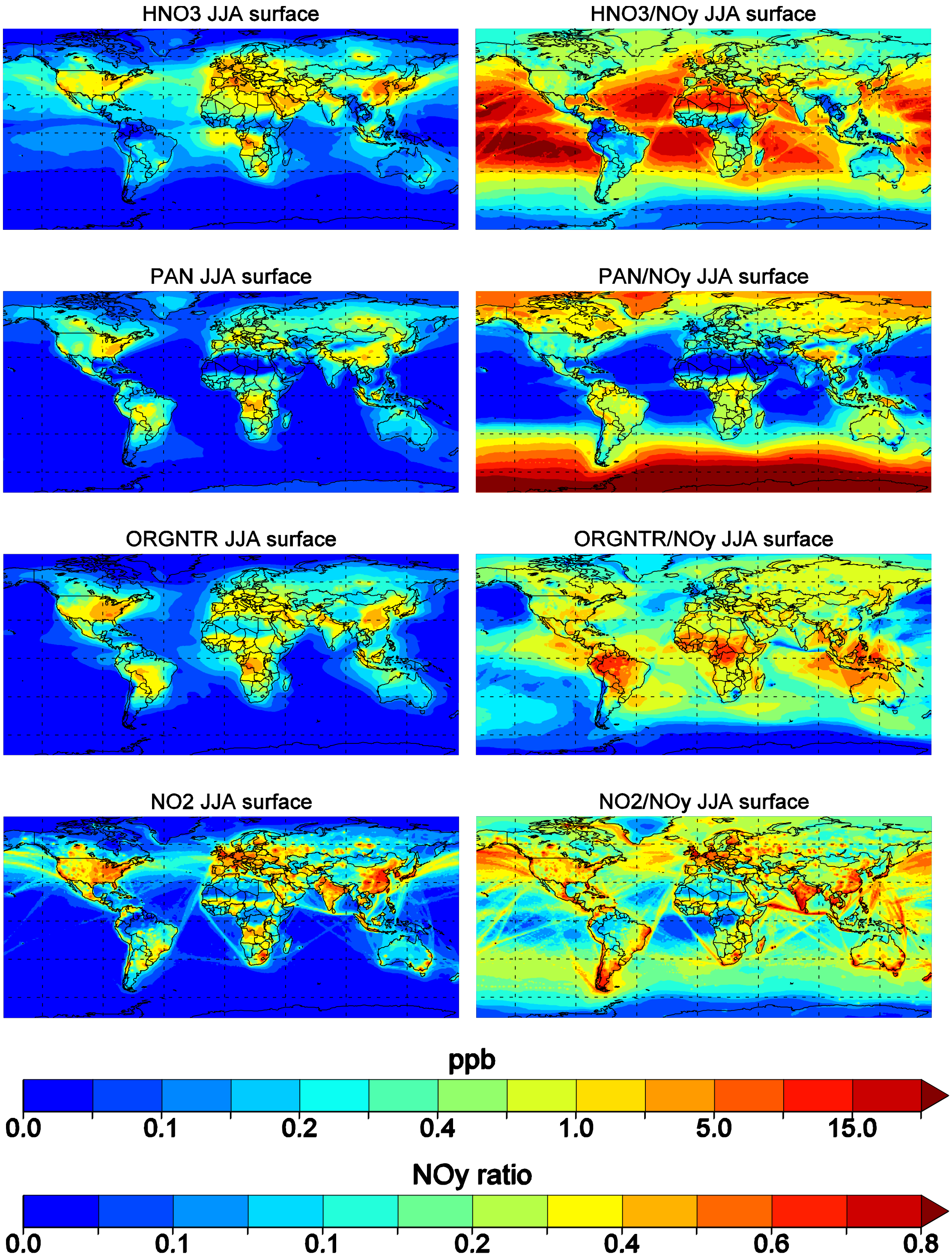

Figure S13: As for Fig S12 except season JJA.

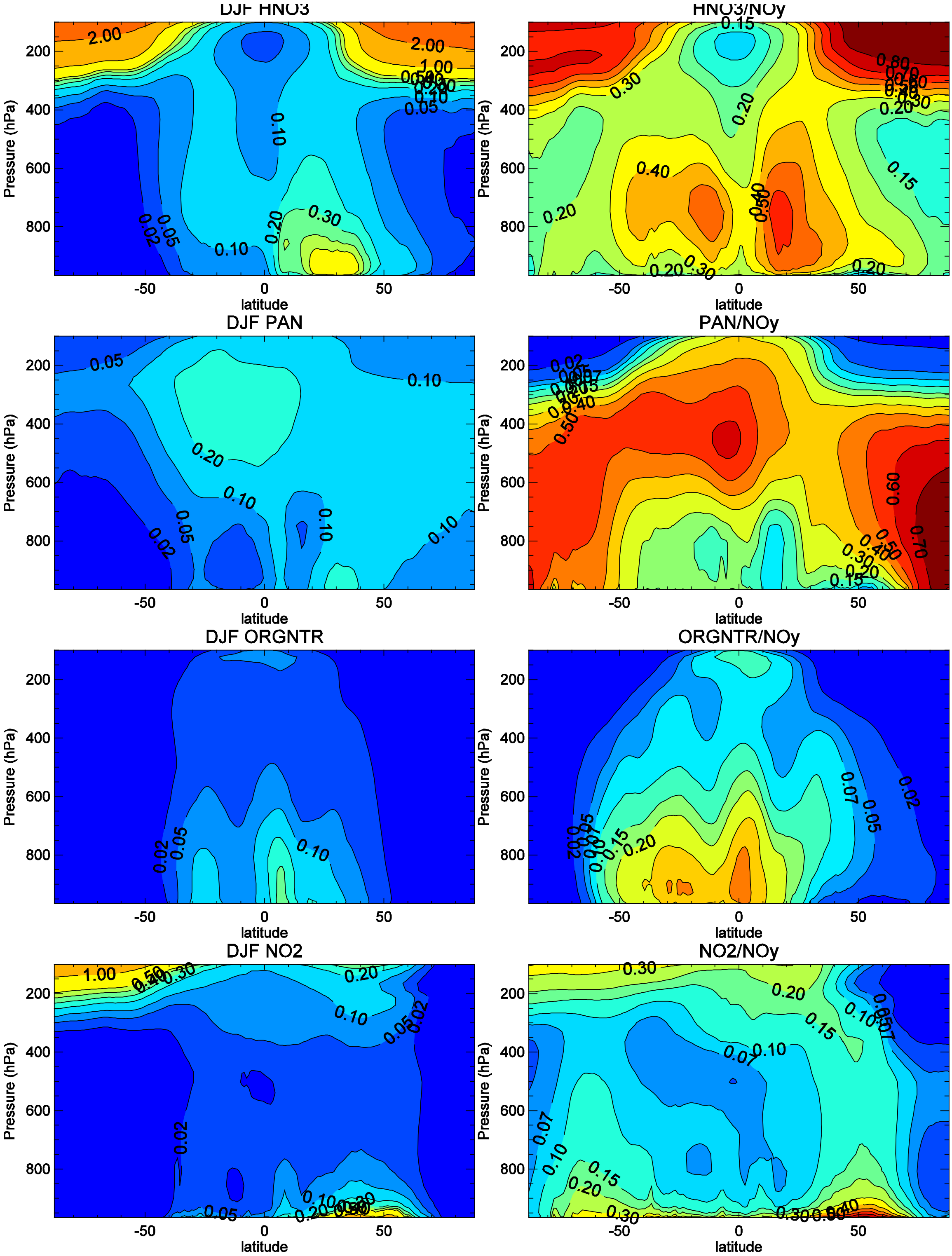

Figure S14: The seasonal zonal mean distribution of (top to bottom) in the 1º x 1º simulation for HNO_3, PAN, ORGNTR and NO_2 for DJF with the corresponding NO_y ratios. The ratio is calculated as [species]/[NOy], where a definition of NOy is given in the text.

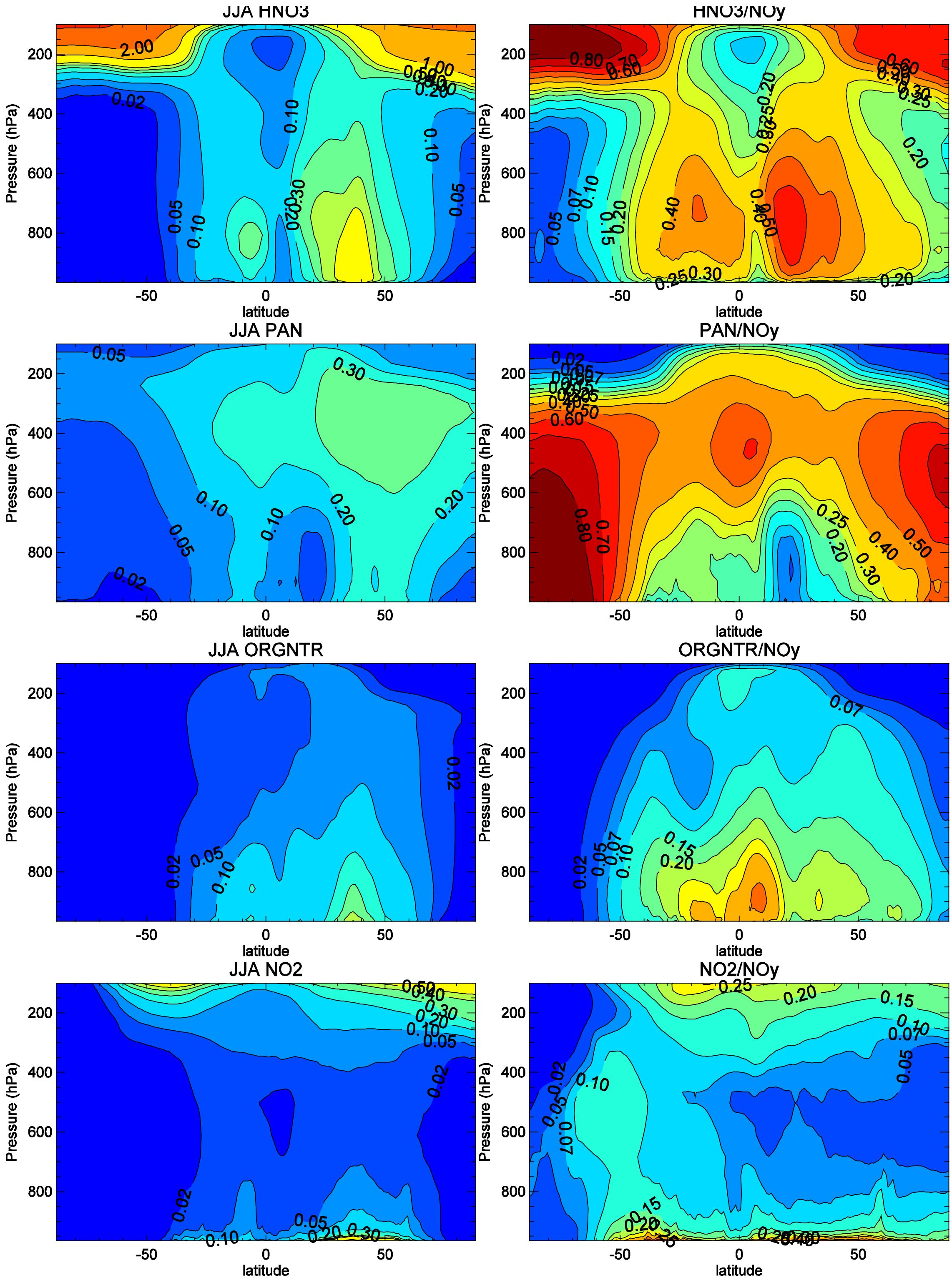

Figure S15: As for Fig. S14 except for season JJA.

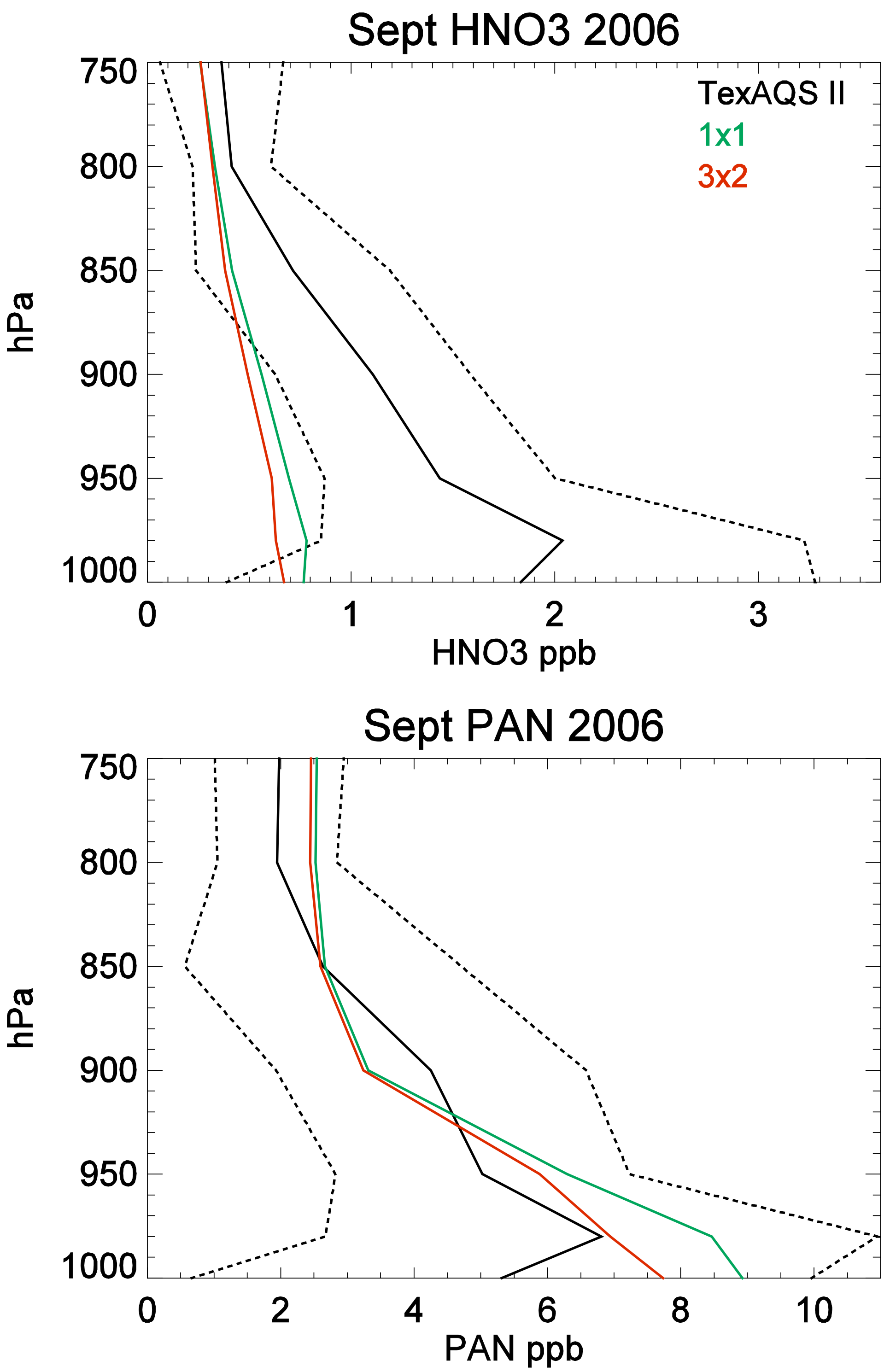

Figure S16: Comparisons of monthly tropospheric HNO_3 (top) and PAN (bottom) profiles during September 2006 above Texas. The 1-σ deviation from the measurements is shown as the dotted line for each species. For details of the flight paths the reader is referred Parrish et al. (2009).

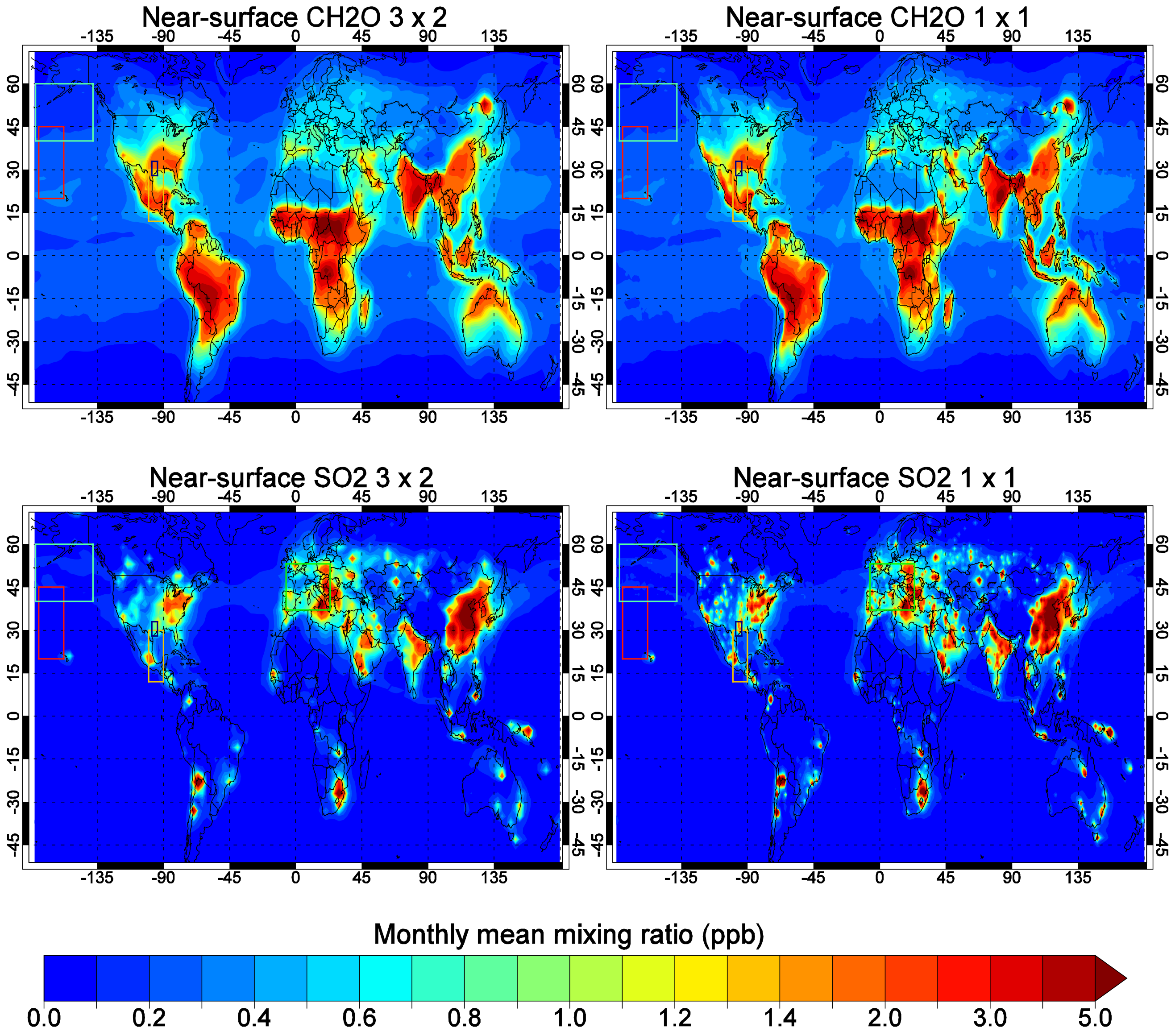

Figure S17: The near-surface distribution in tropospheric CH_2O (top) and SO_2 (bottom) for May 2006 from the 3º x 2º (left) and 1º x 1º (right) TM5-MP simulations. Also shown are the locations of the INTEXB and Texas-AQSII measurement campaigns, and the extent of the EMEP network in the European domain for SO_2 comparisons**.**

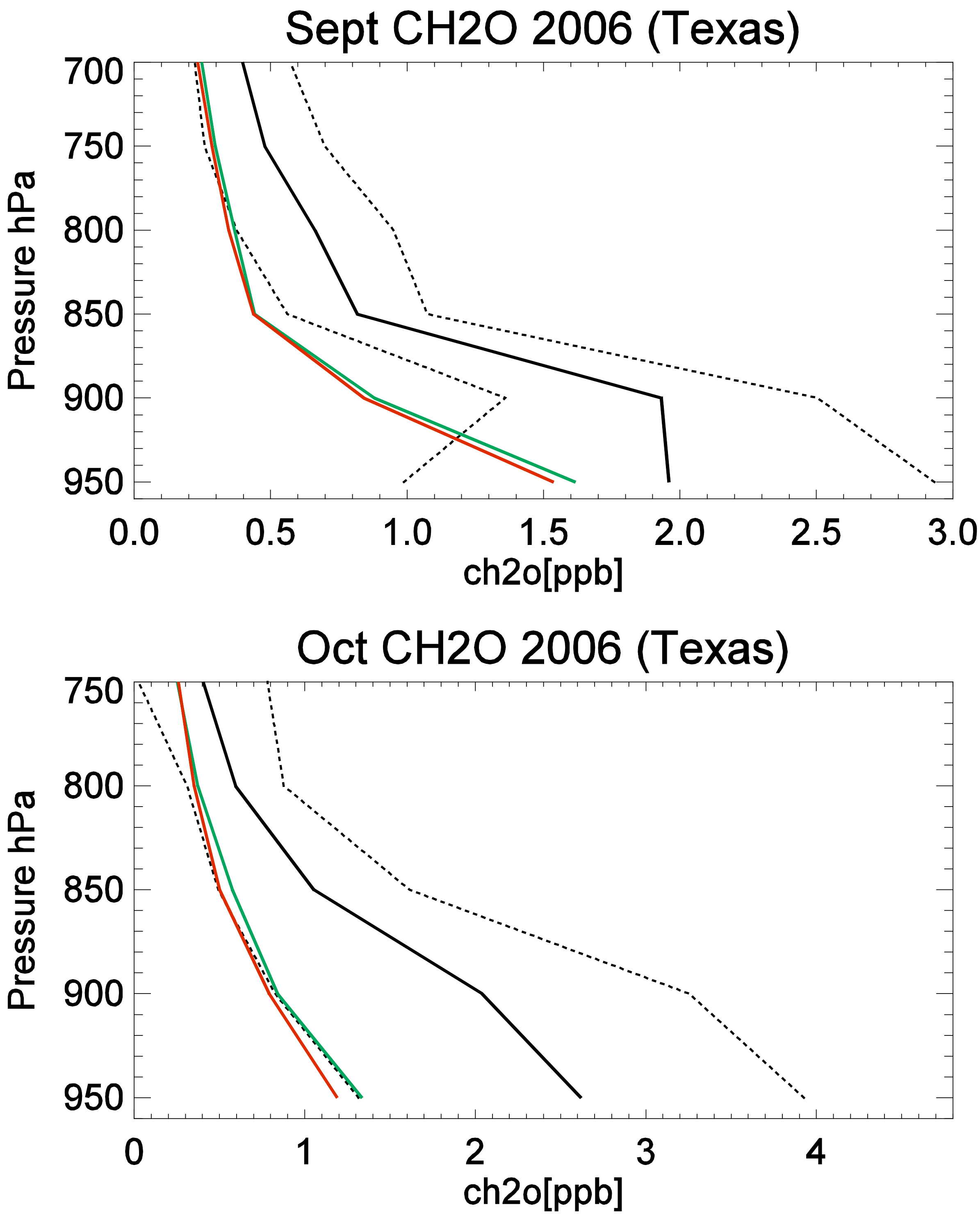

Figure S18: Comparisons of monthly tropospheric CH_2O profiles assembled from data taken during September and October 2006 as part of the Texas-AQS measurement campaign. The 1-σ deviation from the measurements is shown as the dotted line. For details of the flight paths the reader is referred to the details given in Parrish et al. (2009).

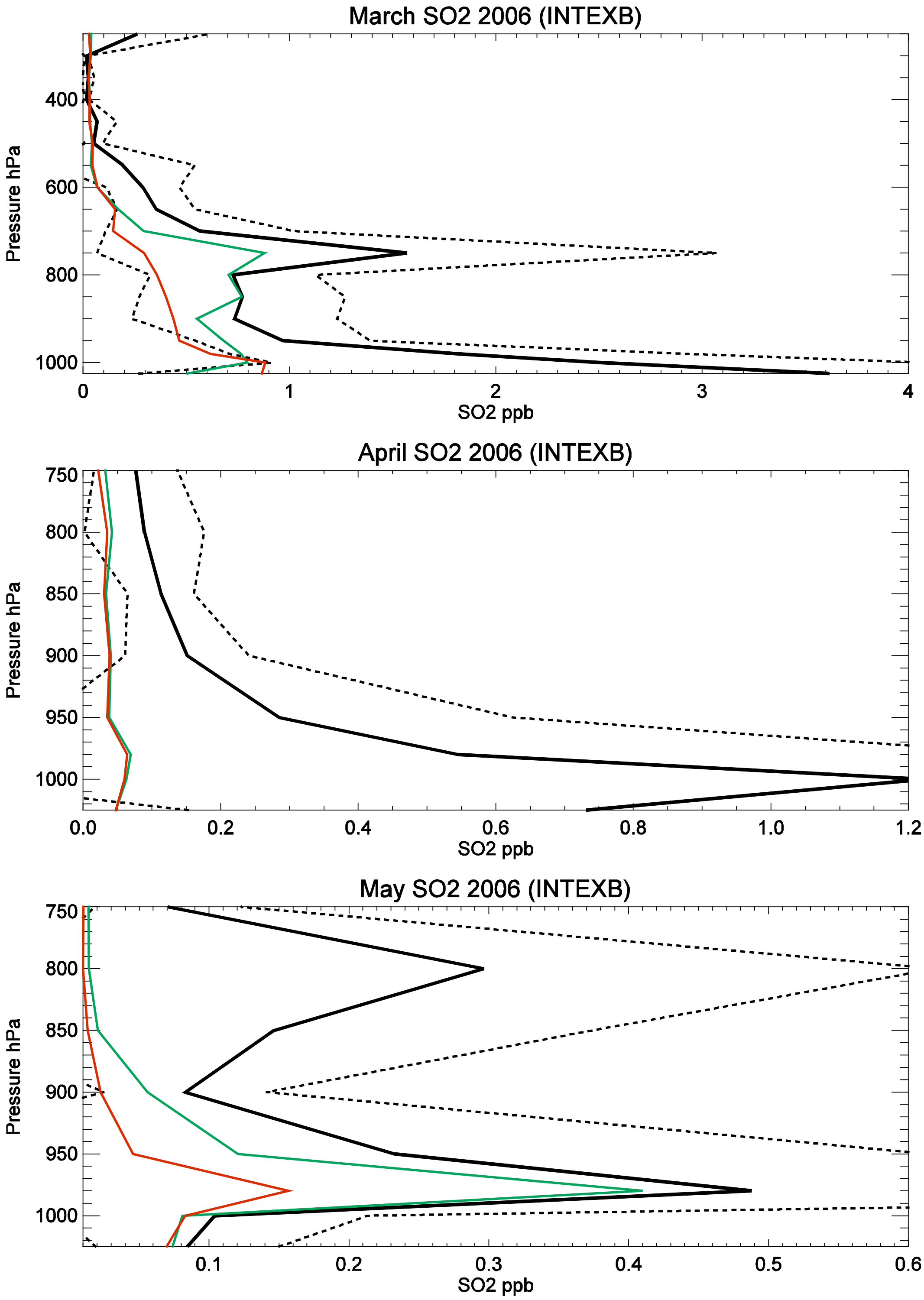

Figure S19: Comparisons of the vertical distribution of SO_2 from both 3°x2° and 1°x1° simulations against measurements made as part of the INTEX B campaign during 2006. The 1-σ deviation from the measurements is shown as the dotted line for each species. For details on the exact location of the flights the reader is referred to Parrish et al. (2009).

Table S1: The tropospheric chemical budget terms for the chemical production (CP), chemical destruction (CD) and accumulated deposition for HNO_3, PAN and ORGNTR given in Tg N yr^{-1} for the 1º x 1º simulation during 2006. Loss of HNO_3 into NO_3^- accounts for the missing HNO_3 loss term. The chemical troposphere is defined according to Stevenson et al. (2006) and fixed across simulations. Percentage differences are given in the parenthesis when compared against the corresponding budget terms from the 3º x 2º simulation (1º x1º/3º x2º). The SH, Tropics and NH are defined as 30-90ºS, 30ºS-30ºN and 30-90ºN, respectively.

Budget Term (Tg/N)	Global	SH	Tropics	NH
Strat. Nudge	0.3	0.1	0.1	0.1
HNO_3 CP	44.0 (0.3)	1.9 (1.0)	22.8 (-1.0)	19.3 (1.7)
HNO_3 CD	6.7 (-4.8)	0.5 (4.7)	3.9 (-2.5)	2.3 (6.7)
HNO_3 Dep.	35.9 (1.5)	2.0 (-0.5)	18.2 (1.6)	15.6 (1.7)
PAN CP	199.1 (-2.4)	7.6 (-3.0)	150.8 (-2.7)	40.7 (-1.1)
PAN CD	197.5 (-2.4)	7.7 (-3.0)	150.2 (-2.7)	39.7 (-1.1)
PAN Dep.	1.6 (2.5)	0.1 (1.0)	0.7 (-0.5)	0.8 (-4.6)
ORGNTR CP	9.8 (-4.8)	0.3 (-3.0)	6.9 (-5.5)	2.6 (-3.4)
ORGNTR CD	4.2 (-4.6)	0.2 (-5.0)	2.9 (-3.4)	1.3 (-0.8)
ORGNTR Dep.	5.7 (-3.6)	0.5 (-2.0)	3.5 (-4.4)	1.8 (-2.8)

Table S2: The tropospheric chemical budget terms for the short-lived N-species HONO, HNO_4 and N_2O_5 (Tg N yr^{-1}) during 2006 for the 1º x 1º simulation. Both HNO_4 and N_2O_5 exist in chemical equilibrium with their respective chemical precursors which accounts for the dominant loss terms (not given), where only oxidation by OH and heterogeneous conversion terms are provided. The chemical troposphere is defined according to Stevenson et al. (2006) and fixed across simulations. Percentage differences are given in the parenthesis when compared against the corresponding budget terms from the 3º x 2º simulation (1º x1º/3º x2º). The SH, Tropics and NH are defined as 30-90ºS, 30ºS-30ºN and 30-90ºN, respectively.

Budget Term (Tg N yr^{-1})	Global	SH	Tropics	NH
HO + NO	22.9 (-3.0)	1.3 (-0.8)	16.4 (-6.4)	5.2 (9.0)
OH + HONO	2.6 (-1.9)	0.1 (-)	1.8 (-5.2)	0.7 (6.3)
HNO_4 CP	168.7 (-1.4)	7.5 (-0.4)	106.4 (-1.2)	54.7 (-1.7)
OH + HNO_4	13.5 (-1.2)	1.1 (0.9)	8.4 (-2.0)	4.0 (-)
N_2O_5 CP	628.4 (12.4)	11.2 (24.9)	322 (12.8)	226 (11.6)
N_2O_5 + aero	6.3 (5.9)	0.1 (14.3)	1.7 (12.0)	4.5 (3.9)
N_2O_5 + cloud	3.2 (-1.9)	0.1 (-)	0.7 (4.8)	2.5 (0.8)
N_2O_5 Dep.	0.3 (-3.0)	-	0.1 (-)	0.2 (-7.5)